June 9, 2003 CBN 03-11

DAMPING RING FOR THE NEXT LINEAR COLLIDER

A.Mikhailichenko[1], Cornell U., LEPP, Ithaca, NY 14853

Abstract

We are presenting some considerations on the damping ring–the source of e^+, e^- for the Next Linear Collider. We are concluding that the simple FODO–like structure operating at ~3GeV is more guaranteed for future collider, than any other one described so far. Considerations include intra—beam scattering, beam and spin dynamics.

INTRODUCTION

One of the first suggestions to use a damping ring as injector for linear collider was made in [1]. In [2] probably the first generalized scheme of damping was represented. Although series of publications emerged soon after this last one, the next step in developing of philosophy for damping ring design was a publication [3]. Here for the first time systematic utilization of wigglers installed in straight sections of a racetrack was described. These wigglers give ~same damping as the one from the bending magnets. Wiggler was considered simply as a series of dipole magnets, however. Contemporary shapes of some damping rings designs for linear colliders are coming from there.

Meanwhile wiggler is very tricky device, so importance of fringe field effects were understood in full only recently. First systematic publication on nonlinear effects in a wiggler is probably [4], however it was not recognized as extremely important issue[2]. On the basis of [4] cautious estimations on influence of wiggler nonlinearities to damping ring performance were made in [5]. In this last publication the NLC scheme analyzed in little bit more details, than original publication [6]. It is interesting, that the authors in [5] mentioned that the damping ring with required parameters could be designed without wigglers at all at higher energy.

Meanwhile at Novosibirsk the main philosophy was namely associated with damping in magnets of as simple magnetic structure as possible [7]. Rich experience was accumulated in dealing with IBS there too. That was primary due to specifics of operation of rings at low energy there.

Looks that published description of damping ring for NLC so far [8] has two difficult places: IBS analyses done at the level not adequate to the scale and cost of the project and, also, description of dynamics in ~60m-long wigglers suffer from multiple assumptions. Spin dynamics is not described at all. Meanwhile polarized electrons (and, possibly, positrons) are the non-questionable parameter of the beams at Next Linear Collider. Designers of the ring for NLC refer sometimes to the CESR-c 18m long wiggler installation. However, despite one purpose of this installation –damping time reduction –is similar to what required for future linear collider, the goal of CESR's installation is to *increase* emittance in contrast with the goal clamed for the damping-ring for LC. In both cases IBS will play important role however.

In this publication we are planning to compare parameters of the rings developed for NLC so far with FODO-like structures similar to the ones developed years ago for VLEPP [9, 10]. We will consider some extreme configurations such as Linear Damping System for example.

---

[1] Phone: (607) 255-3785, Fax: (607) 255-8062, e-mail "mikhail@lns.cornell.edu

[2] One can see this from the post talk questions after presentation [4] was made.

LIMITATIONS FOR EMITTANCE AND NUMBER OF PARTICLES

One can see, that for every scheme of LC remaining under development now, utilization of beams with smaller transverse and longitudinal emittances allow having smaller beam size at IP. So even with lowered bunch population, luminosity can be kept at the same level if emittance reduced. Lowering the number of particles in the bunch makes the beam more stable during acceleration. Lowering the bunch population also reduces a problem with intra-beam scattering phenomena in damping ring-injector.

There is quantum limitation for the lowest emittance in a damping ring as [11]

$$(\gamma\varepsilon_x)(\gamma\varepsilon_y)(\gamma\varepsilon_s) \geq (\tfrac{1}{2})(2\pi\lambda\!\!\!^{-}_C)^3 N\,, \qquad (1)$$

where $\lambda\!\!\!^{-}_C = \hbar / mc = 3.86\cdot 10^{-11}$ cm, $\gamma\varepsilon_s = \gamma l_b(\Delta p_{\|} / p_0)$–is an invariant longitudinal emittance, l_b – is the bunch length, $(\Delta p_{\|} / p_0)$ – the relative momentum spread in the beam, $\gamma\varepsilon_x$ and $\gamma\varepsilon_y$ –are the transverse horizontal and vertical emittances, N is bunch population. For real projects under our interest this limitation is far, however. In damping rings motion is 3D as a requirement for longitudinal stability. One can imaging operation of damping ring at critical energy with appropriately arranged feedback however. In this case the motion becomes a 2D one. For 2D motion, *which happens at critical energy only*, two-dimensional phase space limitations come from (1) to

$$(\gamma\varepsilon_x)(\gamma\varepsilon_y) \geq (\tfrac{1}{2})(2\pi\lambda\!\!\!^{-}_C)^2 N\,. \qquad (2)$$

What is important here, that in formulas (1) and (2) emittances appear as product of ones corresponding to each degree of freedom. One can see, that right side in (2) goes to be $(\gamma\varepsilon_x)(\gamma\varepsilon_y) \geq 2.94\cdot 10^{-20} N$. Typical emittance product for the left side can be suggested as $(\gamma\varepsilon_x)(\gamma\varepsilon_y) \cong 10^{-10}$ cm rad. All N particles must be in one slice, having thickness $\sim\lambda\!\!\!^{-}_C$ however. Meanwhile characteristic distance between particles in the bunch is $\sim l_b / N$. For the number of particles $N\sim 10^{10}$ and bunch length $l_b \cong 0.1$cm, $l_b / N \cong 10^{-11}$ cm i.e. ~single particle per slice, so quantum effects cannot manifest here too.

Minimal number of particles required for collision can be defined as the following. In a moving frame the minimal uncertainty in definition of transverse position can be estimated as a $\lambda\!\!\!^{-}_C$, leaving uncertainty for transverse momentum as mc. Meanwhile spread of transverse momentum for colliding beam at IP is $p_{\perp} \cong mc\gamma\sqrt{\gamma\varepsilon / \gamma\beta_0}$. For typical emittance value $\gamma\varepsilon \cong 10^{-4} cm\cdot rad$, $\gamma \cong 10^6$, $\beta_0 \cong 10^{-2} cm$-beta function at IP, $p_{\perp} \cong mc\cdot 10^2$, i.e. much more than defined by uncertainty. Minimum number of particles N can be found from luminosity required $N^2 \geq 4\pi\lambda\!\!\!^{-2}_C L / n f$, where f is a repetition rate, n is a number of bunches per train. For $L \cong 10^{34}$, f=100Hz, n=10, $N \geq 4\cdot 10^5$. So only half of a million particles is enough for successful operation. With such amount of particles all collective phenomena vanished.

We also mentioned in one of our publications [12], that lowered emittance with reduced number of particles can be obtained by scrapping all extra particles obtained from usual beam injectors. Phase density will remain the same however. So even having in mind these options, it is necessary to (re)consider all possibilities for obtaining as dense beams as possible.

PHYSICAL REQUIREMENTS

Physical requirements for the beam parameters considered in [7], [10]. In this last publication mostly of physical considerations are concluded. Below we will use results obtained there for the first time. First there was understanding that collisions will go with flat beams having significant aspect ratio. In this case magnetic field reduced and defined by large (horizontal) dimension, so radiation on incoming bunch can be suppressed. In that sense radial emittance is not playing crucial role at all. Really, if one fixes the losses by SR due to beamstrahlung

$$\left(\frac{\Delta E}{E}\right)_{max} \cong \frac{8\sqrt{\pi}}{3}\cdot\frac{r_0^3\gamma N^2}{\sigma_x^2\sigma_s}, \tag{3}$$

where σ_x and σ_s are horizontal and longitudinal dimensions respectively, then parameters included in this formula are restrained. Substitute this in formula for luminosity

$$L = \frac{N^2 f H}{4\pi\sigma_x\sigma_y} = \frac{N^2 f \gamma H}{4\pi\sqrt{\beta_x\beta_y\varepsilon_x\varepsilon_y}}, \tag{4}$$

where ε_x, ε_y stand for horizontal and vertical normalized emittances respectively, f stands for repetition rate, H is enhancement parameter, $\beta_{x,y}$ are envelope functions at IP, one can obtain for H=1, $\beta_y \equiv \sigma_s$ required value for vertical invariant emittance as [10]

$$\varepsilon_y \cong \frac{N^2 f^2 (\Delta E/E)_{max}}{L^2 (4\pi)^2 \frac{8}{3}\sqrt{\pi} r_0^3} = 3\cdot 10^{-8}\frac{\left(\frac{N}{10^{11}}\right)^2\left(\frac{f}{10^2}\right)^2\left(\frac{\Delta E/E}{0.8}\right)}{\left(\frac{L}{10^{34}}\right)^2} \text{ [cm rad]}. \tag{5}$$

Substitute here for example $L = 10^{34}$ cm^{-2} s^{-1}, f=100Hz, N=10^{11}, $\Delta E/E = 0.5$, one needs to has vertical emittance as low as $\varepsilon_y \cong 3\cdot 10^{-8}$ cm rad. With such emittance, vertical size of the beam goes to be $\sigma_y = \sqrt{\varepsilon_y\beta_y/\gamma} \cong \sqrt{\varepsilon_y\sigma_s/\gamma} \cong \sqrt{3\cdot 10^{-8}/10^7} \cong 5.5\cdot 10^{-8}$ cm for $\sigma_s/\gamma \cong 10^{-7}$.

For arrangements of $\gamma-\gamma$ collisions emittances of electron beams serving for further conversion into Compton gammas must be lower than

$$\varepsilon_x \cong \varepsilon_y \le \frac{l^2}{\beta\gamma}, \tag{6}$$

where β is an envelop function value at IP, l is the distance between conversion point ant collision point for gammas, as the secondary photons distributed within angle $1/\gamma$. One can see, than requirements to the radial emittance become tighter, while requirements to the vertical emittance released. For luminosity ~10^{33} cm^{-2} s^{-1}, l=10 cm and $\beta \cong 0.1$ cm this will require emittances ~5 mm mrad [10].

For longitudinal emittance $\varepsilon_{\parallel} = \gamma\sigma_s\frac{\Delta E}{E}$ energy spread must be within acceptance of final focus system. In its turn the energy spread defined by energy distribution introduced by BNS mechanism. For fixed monochromaticity at the level $\Delta E/E \le 0.5\%$, the length of the bunch must be [10]

$$\sigma_s \cong \frac{N}{10^{12}} \text{ [cm]} . \tag{7}$$

All together define the longitudinal emittance as $\varepsilon_{\|} = 5 \cdot 10^{-15} \gamma N$.

Polarization of collided beams was recognized as a crucial parameter from the very beginning, so all collisions arranged as both (electrons and positrons) polarized.

Physical parameters required for successful collisions summarized in Table 1 below. These parameters represented here for 100 Hz operation do not depend on any detailed scheme.

Table 1.

Parameter	Units	e^+e^-	e^+e^-	$\gamma-\gamma$
Luminosity, L	$cm^{-2}\ s^{-1}$	10^{33}	10^{34}	10^{33}
Bunch population, N	$2\ 10^{11}$	1	1	1
Bunch length, σ_s	cm	0.1	0.1	0.1
Radial beta-function, β_x	cm	10.	10.	1.0
Vertical beta-function, β_y	cm	0.1	0.1	1.0
Vertical size at IP, σ_y	μm	0.004	0.0004	0.06
Horizontal size at IP, σ_x	μm	2.0	2.0	0.06
Vertical norm. emittance, ε_y	cm rad	3×10^{-6}	3×10^{-8}	8×10^{-5}
Horizontal norm. emittance, ε_y	cm rad	8×10^{-3}	8×10^{-3}	8×10^{-5}
Final lens vibration restrain	μm	0.02	0.002	0.1

These parameters give an idea about physical restrains and requirements.

DAMPING TIME

Ratio of emittances for extracted/injected beam define the time required for cooling the energy spread and emittance as the following

$$\tau_s \cong \frac{2}{f} \frac{1}{ln(\varepsilon_{in} / \varepsilon_{ext})}, \tag{8}$$

where ε_{in} stands for initial (injected) emittance and ε_{ext} for final (extracted) one. So for strong focusing machine, the last formula (8) yields the following relations between the partial damping times

$$\tau_x \cong 2\tau_s \cong \tau_y \cong \frac{2E}{< P_\gamma >} = \frac{3mc^2}{r_0^2 \gamma c < H_\perp^2 >} \cong \frac{3}{r_0 \gamma^3 c \left\langle \frac{1}{\rho^2} \right\rangle}, \tag{9}$$

where $H_\perp(s)$ is magnetic field value along longitudinal coordinate s, ρ is a current bending radius, $P_\gamma(s) = \frac{2}{3} r_0^2 \gamma^2 c H_\perp^2(s) = \frac{2}{3} e^2 \gamma^4 c / \rho^2$ is power of radiation. Formula (9) defines the share of period occupied by wigglers as

$$\eta \cong \frac{l_W}{\Pi} \cong 6\frac{mc^2}{r_0^2 \gamma c < H_\perp^2 > \tau_y} \quad , \tag{10}$$

where l_W is the wiggler length, Π is perimeter of damping ring, and it was used that average of magnetic field square is a half of its amplitude value. Substitute here $\tau_s \cong 4$ ms ([8] NLC), $\gamma \cong 3000$, H_{W0}=20kG, one can estimate $\eta \cong 0.43$ if wigglers are dominating in a damping.

It was mentioned in [10], however, that it is difficult to obtain designed spatial field distribution as the iron is saturated and the field is sensitive to the wire locations. That was identified as a main source of uncertainties. We will discuss this subject lower.

PROCESSES IMPORTANT FOR THE BEAM EMITTANCE

Since the very beginning of linear collider activity more than a quarter century ago, the basic philosophy in approach to this problem was in equalizing RMS input to the emittance growth rate from intra-beam scattering and from quantum fluctuations for the beam prepared in the damping ring-injector. The input from quantum fluctuations to the emittance associated with very simple mechanism, however. Sudden energy change by particle due to radiation of quanta at the place where dispersion is not zero, instantly transferees this energy jump into the transverse displacement from new equilibrium orbit. Thus, the schemes of cooling rings with lowest possible dispersion at places with highest radiation (wigglers, magnets) were developed to lower this input.

Quantum fluctuations

In the assumption of statistically independent emission of quants by particle equilibrium energy spread defined by the balance

$$\left(\frac{\Delta E}{E}\right)_\gamma^2 = \frac{1}{4}\left\langle \dot{N} \cdot \left(\frac{\varepsilon_\gamma}{E}\right)^2 \right\rangle \cdot \tau_s \tag{11}$$

where ratio of instant quantum energy to the full one defined (see for example [13])

$$\dot{N} \cdot \left(\frac{\varepsilon_\gamma}{E}\right)^2 = \frac{55}{2^3 3^{3/2}} \frac{r_0 \lambda\!\!\!^{-}_C \gamma^5 c}{|\rho|^3} . \tag{12}$$

So the energy spread goes

$$\left(\frac{\Delta E}{E}\right)_\gamma^2 = \frac{55}{64\sqrt{3}} \frac{e\hbar\gamma}{m^2c^3} \frac{\left\langle |H_\perp|^3 \right\rangle}{\left\langle H_\perp^2 \right\rangle} = \frac{55}{64\sqrt{3}} \lambda\!\!\!^{-}_C \gamma \frac{\left\langle \frac{1}{|\rho|^3} \right\rangle}{\left\langle \frac{1}{\rho^2} \right\rangle} . \tag{13}$$

Instant radiation of quantas yield emittance growth defined by

$$\frac{d\varepsilon_{x,y}}{dt} \cong \left\langle \left(H_{x,y} + \frac{\beta_{x,y}}{\gamma^2} \right) \frac{d(\Delta E / E)_{tot}^2}{dt} \right\rangle - 2\alpha_{x,y}\varepsilon_{x,y} , \tag{14}$$

where dispersion invariant defined as

$$H_{x,y} = \frac{1}{\beta_{x,y}}\left(\eta_{x,y}^2 + (\beta_{x,y}\eta'_{x,y} - \frac{1}{2}\beta'_{x,y}\eta_{x,y})^2\right), \tag{15}$$

$\eta_{x,y}$ –are dispersion functions. Partial decrements $\alpha_{x,y,s}$ defined as $\alpha_i = \frac{J_i}{2\tau_s}$, where $J_x \cong 1, J_y = 1, J_s \cong 2,\ J_x + J_s = 3$. Partial decrement for energy spread is the same as for emittance. In formula (14) the rate of energy spread growth includes additive component from IBS, see lower.

$$\frac{d(\Delta E/E)^2_{tot}}{dt} = \frac{d(\Delta E/E)^2_{IBS}}{dt} + \frac{d(\Delta E/E)^2_{\gamma}}{dt} - \alpha_s\left(\frac{\Delta E}{E}\right)^2, \tag{16}$$

For vertical motion the terms in (14) associated with dispersion invariant are much smaller, than the ones arising from the opening angle β_y/γ^2, indeed for radial motion the terms associated with opening angle are much smaller, than from dispersion invariant. For equilibrium emittance defined by quantum fluctuations only one can obtain

$$\varepsilon_x \cong \frac{55}{64\sqrt{3}}\lambda\!\!\!^{-}_C\gamma^3\frac{\left\langle\left(H_x + \frac{\beta_x}{\gamma^2}\right)\cdot\frac{1}{|\rho|^3}\right\rangle}{\left\langle\frac{1}{\rho^2}\right\rangle}\ ,\quad \varepsilon_y \cong \frac{55}{64\sqrt{3}}\lambda\!\!\!^{-}_C\gamma^3\frac{\left\langle\left(H_y + \frac{\beta_y}{\gamma^2}\right)\cdot\frac{1}{|\rho|^3}\right\rangle}{\left\langle\frac{1}{\rho^2}\right\rangle} \tag{17}$$

Basic way to minimize horizontal emittance is in minimization of dispersion invariant (15) in bending magnets, where $1/\rho \neq 0$.

For the system having period with a focusing quadrupole and bending magnet with defocusing gradient in approximation of thin lens one can obtain [10]

$$\left\langle H_x\frac{1}{|\rho^3|}\right\rangle \equiv \int_0^{2l} H_x\frac{ds}{|\rho^3|} \cong \frac{1}{2l\beta_x}\left(\frac{1}{10}\frac{(l_M/2)}{\rho^2} + \frac{\beta_x^2}{3}\frac{(l_M/2)^3}{\rho^2}\right)\frac{1}{|\rho^3|} \tag{18}$$

where l_M is the length of the magnet and l is a distance between the magnet and lens (so period has the length $2l$) . One can see from here that there is an optimal value for β_x

$$\beta_{xopt} \cong l_M\sqrt{\tfrac{3}{80}},$$

which delivers to the integral (18) value

$$\left\langle H_x\frac{1}{|\rho^3|}\right\rangle \cong \frac{1}{64}\frac{l_M^4}{l|\rho^5|} \cong \frac{1}{4}\frac{l^3}{\rho R^4}, \tag{19}$$

where the last values estimated as $l_M \cong l$, $\rho \cong R/4$, $R \cong \Pi/2\pi$. Substitute this integral into (17) one can obtain minimal emittance value

$$\varepsilon_x \cong \tfrac{1}{2}\lambda\!\!\!^{-}_C\gamma^3\left(\frac{l}{R}\right)^3\ . \tag{20}$$

For the damping time of vertical oscillations one can obtain under these assumptions

$$\tau_y \cong \tfrac{3}{4}\frac{R^2}{r_0 c\gamma^3} \tag{21}$$

Dependence on parameters has fundamental sense so we shall derive it in a different way. From electrodynamics it is known, that at the length of formation $\sim\rho/\gamma$ electron radiates $\sim\alpha = e^2/\hbar c$ photons, which means, that the number of radiated photons per one revolution is $\sim 2\pi\rho\alpha/(\rho/\gamma)\cong 2\pi\alpha\gamma$. As the characteristic frequency in bending magnet goes to be $\frac{3}{2}c\gamma^3/\rho$, then the energy carried out by these photons by turn is $\Delta E_{turn}\cong 3\pi c\alpha\gamma^4/\rho$ and the time for re-radiation all initial energy goes to be $\tau\cong\frac{E}{\Delta E_{turn}}\frac{R}{c}\cdot\cong\frac{mc^2\gamma\rho}{3\pi\alpha c\gamma^4}\frac{R}{c}\approx\frac{R^2}{r_0 c\gamma}$ in agreement with (21).

As one can see from (20), emittance is going down with the number of periods in cubic power. The distance between lenses defined by maximal achievable gradient. For the lens having focal distance $F\cong l/2$ with the length $l_Q\cong F/2$

$$l\cong\frac{2.8}{\sqrt{eG/mc^2\gamma}}\cong 100\cdot\sqrt{\frac{\gamma}{G[Gs/cm]}},$$

so the minimal emittance (20) can be evaluated as

$$\varepsilon_x\cong 1.4\cdot 10^{-2}\frac{1}{(\tau_x[s]\cdot G[Gs/cm])^{3/2}}. \qquad (22)$$

One can see that this estimation does not depend on energy and radius. These last connected for this ring by the following

$$R[cm]\cong 0.1\cdot\gamma^{3/2}\tau^{1/2}[s].$$

So quantum fluctuations require, that for emittance reduction energy must be kept as low as possible. Intrabeam scattering becomes more dominant there, however.

Intra Beam Scattering

Collisions inside moving bunch equalize temperature, however the same processes responsible for the shortening of a beam lifetime [14]. The temperature can be expressed as the following (see for example [15])

$$\tfrac{3}{2}Nk_BT\cong N\cdot mc^2\gamma\left[\frac{\gamma\varepsilon_x}{\beta_x}+\frac{\gamma\varepsilon_y}{\beta_y}+\gamma\left(\frac{1}{\gamma^2}-\langle\psi\rangle\right)\left(\frac{\Delta p_{\|}}{p_0}\right)^2\right], \qquad (23)$$

where $\psi=\frac{\gamma}{l}\frac{\partial l}{\partial\gamma}$. Longitudinal part of temperature has this form because the longitudinal mass is $\frac{1}{m_{\|}}=\frac{1}{m\gamma}\left(\frac{1}{\gamma^2}-\alpha\right)$, $\alpha=\left\langle\frac{\gamma}{l}\frac{\partial l}{\partial\gamma}\right\rangle$. One can see, that this mass defined for the motion accomplished in a revolution over period. In damping rings developed as injectors for future linear colliders, typical values are $\beta_{x,y}\cong 10\text{m}$, $l_b\cong 1\text{cm}$, $\Delta p/p\cong 5\cdot 10^{-4}$, $\gamma\varepsilon_s\cong 3\,\text{cm}$, $\gamma\varepsilon_x\cong 3\cdot 10^{-4}\,\text{cm rad}$, $\gamma\varepsilon_y\cong 3\cdot 10^{-6}\,\text{cm rad}$. This gives $\frac{3}{2}k_BT\cong mc^2\gamma[3\cdot 10^{-7}+3\cdot 10^{-9}+4\cdot 10^{-11}]$. One can see that despite the longitudinal emittance is the biggest one, the longitudinal temperature is the lowest one. This yields the possibility for redistribution the temperatures. One other peculiarity seen from (23) is

that above critical energy longitudinal temperature becomes negative what means that equilibrium is not possible there.

Other important moment is that during equalizing the vertical emittance becomes rising even without coupling due to imperfections of magnetic structure.

In a moving frame velocity of transverse motion can be expressed by simple formula

$$\frac{dp'^2}{dt'} = \frac{4\pi e^4 n' Ln_C}{v'}, \tag{24}$$

where $Ln_C = ln\frac{a_{max}}{a_{min}} \cong ln\sqrt{\frac{(v'/c)^6}{4\pi r_0^3 n'}}$ is Coulomb's integral, n' is the density in moving frame, v' stands for speed of transverse motion in moving frame. Transforming (24) in Lab frame one can obtain diffusion speed as the following [10]

$$\frac{d\left(\Delta p_{\|}/p\right)^2}{dt} \cong \frac{d\left(\Delta E/E\right)^2}{dt} = \sqrt{\frac{2}{\pi}} \frac{Ln_C N r_0^2 c}{\gamma^3 \varepsilon_x \cdot \sqrt{\varepsilon_s \beta_s}\sigma_s \cdot \sqrt{1+\frac{\left(\eta \Delta p_{\|}/p\right)^2}{\varepsilon_x \beta_x}}}. \tag{25}$$

For description of emittance dynamics this expression must be substituted in (14), (16).
For simplest FODO structure solution of (14) ,(17) can be expressed as

$$\varepsilon_x \cong l \cdot \left(\frac{N r_0^2 c \tau_x Ln_C}{4\kappa_0 \gamma^3 \sigma_s R^2}\right)^{0.4}, \tag{25}$$

where coefficient $\kappa_0 = \sqrt{\varepsilon_y/\varepsilon_x}$ defined the coupling arising from hardware imperfection. We would like to attract attention that in mostly publications under this name now in use squares of this value. So the IBS generates coupling what is, according to (14)

$$\kappa_{IBS}^2 \cong \frac{\left\langle \beta_y \right\rangle}{\gamma^2 \left\langle H_x \cdot \sqrt{\frac{1}{\beta_y}} \right\rangle}. \tag{26}$$

For FODO structure this can be estimated as $\kappa_{IBS} \cong \frac{R}{\gamma l}$. Geometrical coupling defined by rotation of quads by random angle within amplitude ϑ_0. If the phase shift for betatron oscillations is not small, then the coupling arisen from *M* periods can be majoretted for our model by

$$\kappa_0 \cong \vartheta_0^2 2M \cong \vartheta_0^2 \frac{2\pi R}{l}. \tag{27}$$

So resulting coupling coefficient comes to

$$\kappa^2 = \kappa_0^2 + \kappa_{IBS}^2.$$

For vertical emittance

$$\varepsilon_y \cong \left(\frac{Nr_0^2 c\tau_x Ln_C}{4\gamma^3\sigma_s R^2}\right)^{0.4} \gamma\cdot l\cdot\left(\kappa_0^2+\kappa_{IBS}^2\right)^{0.8} =$$

$$=\left(\frac{Nr_0^2 c\tau_x Ln_C}{4\gamma^3\sigma_s R^2}\right)^{0.4} \gamma\cdot l\cdot\left(\vartheta_0^2\, 2\pi R l^{1/4}+\frac{R^2}{\gamma l^{3/4}}\right)^{0.8}. \qquad (28)$$

In this case there is an optimal number of periods corresponding minimum in (28) [10]

$$l_{opt}\cong 0.5\frac{R}{(\gamma\vartheta_0)^2},$$

which gives

$$\varepsilon_{opt}=\left(\frac{Nr_0^2 c\tau_x Ln_C}{\sigma_s}\right)^{0.4} 2.73\frac{\vartheta_0^{0.6}}{\gamma^{0.8}}. \qquad (29)$$

So one can see, that accuracy of installation become crucial issue in obtaining small vertical emittance. One can obtain from here that for obtaining vertical emittance ε_{y0} energy of the ring must be

$$\gamma\cong\left(\left(\frac{Nr_0^2 c\tau_x Ln_C\sqrt{R}}{\sigma_s}\right)^{0.4} 2.73\frac{\vartheta_0^{0.6}}{\varepsilon_{y0}}\right)^{1/0.8}. \qquad (30)$$

For example if $\varepsilon_{y0}\cong 0.05$mm mrad , $N=2\cdot 10^{11}$, then $E=mc^2\gamma\cong 1.8$GeV for $\sigma_s\cong 0.5$ cm, R=25 m and $Ln_C\cong 40$. For a damping ring having perimeter 160 m and energy~3.8 GeV optimal number of periods M goes to be M~100 yielding normalized emittance $\varepsilon_y\cong 0.002$mm mrad.

and Resulting emittance, due to IBS, including lifetime, were calculated with two different numerical codes. For each particular structure considered below results include these numerical modeling. One group of codes tested with existing rings at BINP [7].

Dynamic aperture

As always, for compensation of chromaticity of quadrupole the sextupoles are used in places, when dispersion has nonzero value. In BEP machine the profile of the quadrupoles was modified so that the quad acquires controllable sextupole component [7]. Basic requirement is that the focal distance of the quad and sextupole

$$F\cong\frac{\int\left(G(s)+\frac{\partial H(x,s)}{\partial x^2}\cdot\eta\frac{\Delta p}{p}+\ldots\right)ds}{(HR)\cdot\left(1+\frac{\Delta p}{p}+\ldots\right)} \qquad (31)$$

become not a function of momentum if $G/\psi=H''$. From the other hand the particle, while passing the sextupole at the distance x from axis, acquires the angular kick

$$\Delta x' \cong \frac{\int H'' \cdot ds}{(HR)} \cdot \frac{x^2}{2} \cong \frac{\int G \cdot ds}{(HR)\eta} \cdot \frac{x^2}{2} \approx \frac{x^2}{2F\eta} \tag{32}$$

This value must be compared with angular spread in the beam as $x' \cong \sqrt{\frac{\varepsilon_x}{\gamma\beta_x}}$, so

$$\frac{x^2}{2F\eta} \equiv \frac{x}{2F\eta}\sqrt{\frac{\varepsilon_x\beta_x}{\gamma}} \le \sqrt{\frac{\varepsilon_x}{\gamma\beta_x}}, \tag{33}$$

and majorette for the aperture comes to [7,10]

$$x_{max} \le \frac{2F\eta}{\beta_x}. \tag{34}$$

For typical FODO structure $\beta / F \cong 4.8$ (for $\Delta\mu = \pi/2$) so $x_{max} \cong 0.4\eta$. One can see, that desire to have as low dispersion as possible for minimization of invariant (15) forces shrinkage of dynamic aperture.

With the same accuracy the maximal acceptance can be estimated as

$$\varepsilon_A \cong \gamma\frac{x_{max}^2}{\beta_{x\,min}} = \gamma\frac{0.16\eta^2}{\beta_{x\,min}} \cong \frac{l^3}{R^2}\left(\frac{\beta_{min}}{\beta_{max}}\right)^{3/2} \tag{35}$$

All these processes were modeled with numerical code, and results are represented below for some particular structures. Details, again one can find in [10]. General conclusion made there is that for energy of the ring below 3.5 GeV it is possible to reach conditions when dynamic aperture not limiting acceptance of the ring.

For calculations of dynamic aperture and phase space characteristics numerical code was used. It starts particle beginning from large aperture and tracks it through the structure. If particle is lost, new start coordinate, smaller, than previous one injected and so on. Some results are represented in Figs. 3, 6, 9.

Consideration of IBS showed, that minimal value of coupling could be reached as low as $\varepsilon_y / \varepsilon_x \cong 10^{-4}$. Namely this value defines the geometrical limit for coupling. Accuracy of sextupole alignment must be <6μm, quadrupole tilt <0.3 mrad [10].

MAIN TYPES OF STRUCTURES

During the times for VLEPP activity, few designs of damping rings were considered. Among them there are FODO structure, BEP-type structure and Chasman-Green-like one.

FODO structure

Example of mechanical realization of magnetic structure of FODO type is represented in Figure1. Here the magnet, quadrupole and sextupole installed on thick Aluminum plate. All these elements aligned to the reference points at the plate with micrometer accuracy. Vacuum chamber aligned with respect to the magnetic center of quadrupole. Pick-up electrodes calibrated in advance for having zeros coinciding with magnetic center of quads, similar as it was done for FFTB. Further only plates will be aligned at the place. The straight sections ~80 cm are long enough for installation of RF cavities, injection/extraction elements etc.

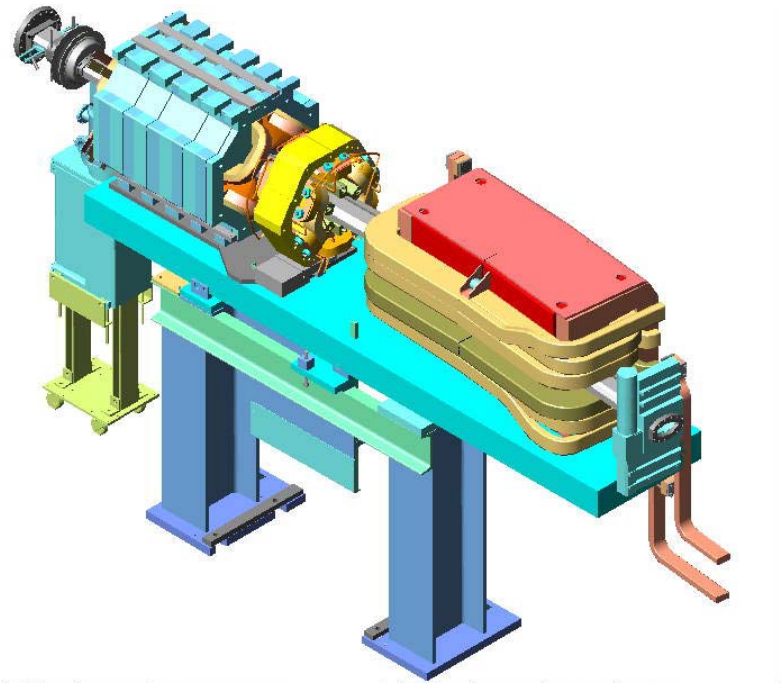

Figure 1: One period of FODO structure.

Vacuum supported by getter pumps and magneto-discharge pumps. Vacuum chamber made from copper. Technology for preparation of the vacuum chamber is basically the same as for preparation of room temperature accelerating structure. So it is exposed to the air only for a limited time. Some optics parameters of the ring are represented in Table 2.

Table 2.

Energy	~3 GeV
Length of magnet	80 cm
Field in magnet	~15.15 kG
Gradient in magnet	~ -1.7kG/cm
Sextupole in magnet	-0.59 kG/cm^2
Length of focusing quad	80 cm
Gradient	~1.7 kG/cm
Sextupole	0.15 kG/cm^2
Straight sections	80 cm
Perimeter	~160 m
Number of periods	50

This structure tuned for $Q_x \cong 18.54$, $Q_y \cong 18.49$, $\tau_y \cong 3.2$ ms. For RF voltage ~2 MeV $\sigma_s \cong 1$ cm. Beam lifetime for 10^{10} particles is ~7.7s. For mechanical coupling $\kappa_0 = 0.02$ vertical invariant emittance goes to $\sim \varepsilon_y \cong 8.6 \cdot 10^{-10}$ m rad. Other parameters are represented in Table 5.

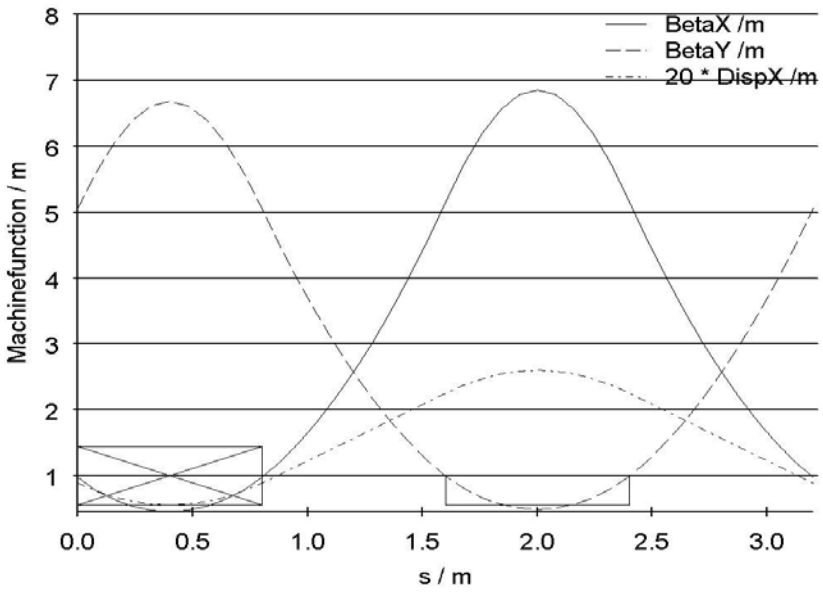

Figure 2: Machine functions of FODO structure. Maximum value of dispersion function is ~12.5cm.

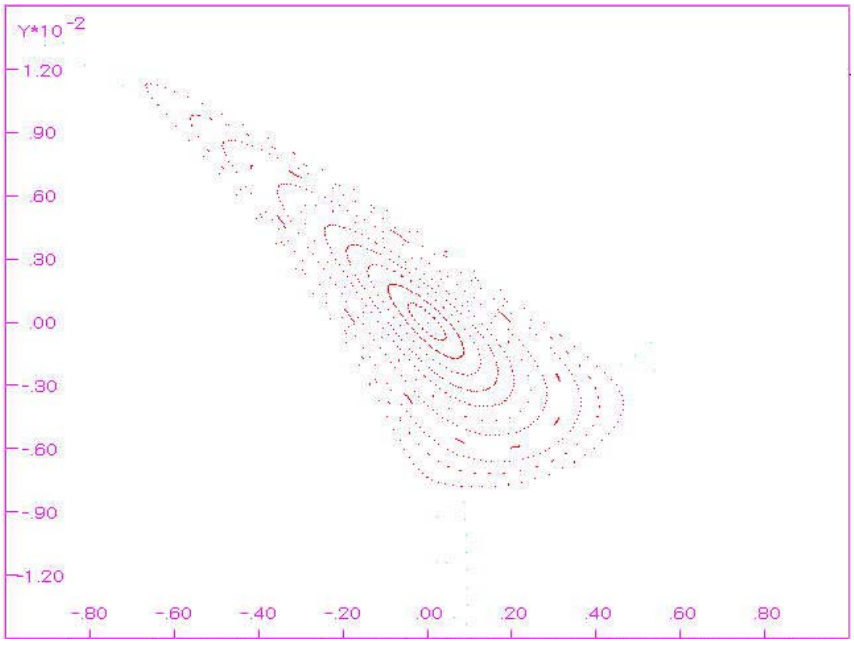

Figure 3: Phase space portrait at the magnet entrance. Abscissa represents x, cm, ordinate x' rad, respectively.

Exact shape of phase portrait depends on current position of working point on the tune plane, however.

BEP like structure.

In this structure, [7], the defocusing field represented by separate lens installed close to the magnet, Figure 4. In this case magnet becomes much simpler, however additional lens emerges. Sextupoles implemented in the pole profile as it was done in real working prototype [7]. Additional trim sextupoles, skew quads and skew sextupoles installed in straight sections (not shown in Figure 3).

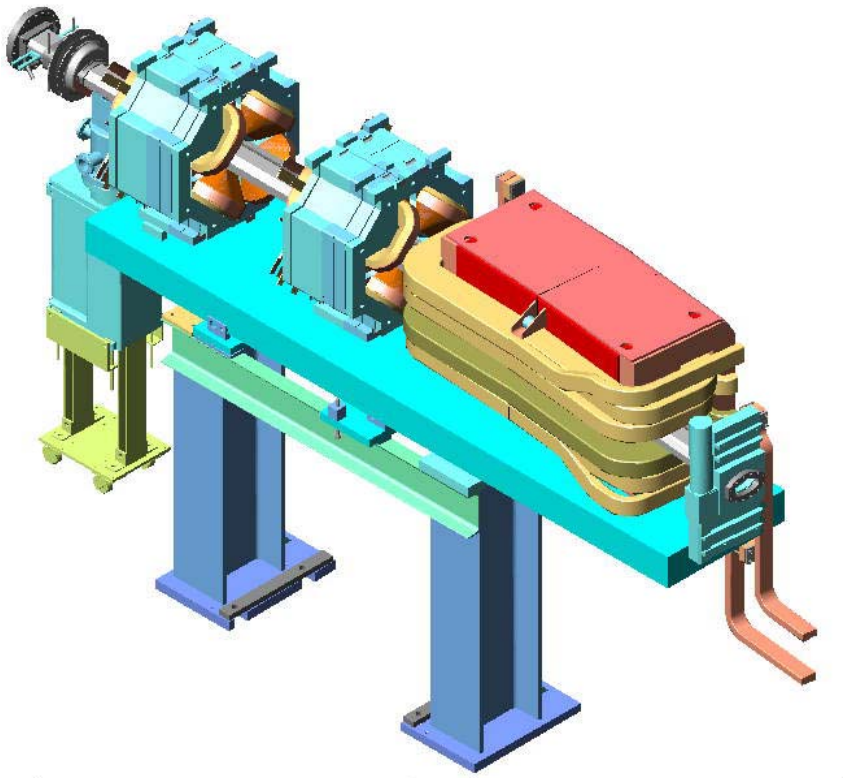

Figure 4: Mechanical realization of BEP-like structure period.

Technology of alignment is basically the same as for FODO one described above. Thick Al plate now carries additional lens. For this structure the accuracy of vertical alignment of the magnet becomes relaxed due to absence of any focusing properties.

Table 3.

Energy	~3 GeV
Length of magnet	60 cm
Field in magnet	~15.15 kG
Length of defocusing quad	30cm
D Gradient	~ -5.56
Sextupole in lens	-1.5 kG/cm^2
Length of focusing quad	30 cm
F Gradient	~5.7 kG/cm
Sextupole in lens	0.7 kG/cm^2
Distance between lenses	30 cm
Straight section	110 cm
Perimeter	~181 m
Number of periods	66

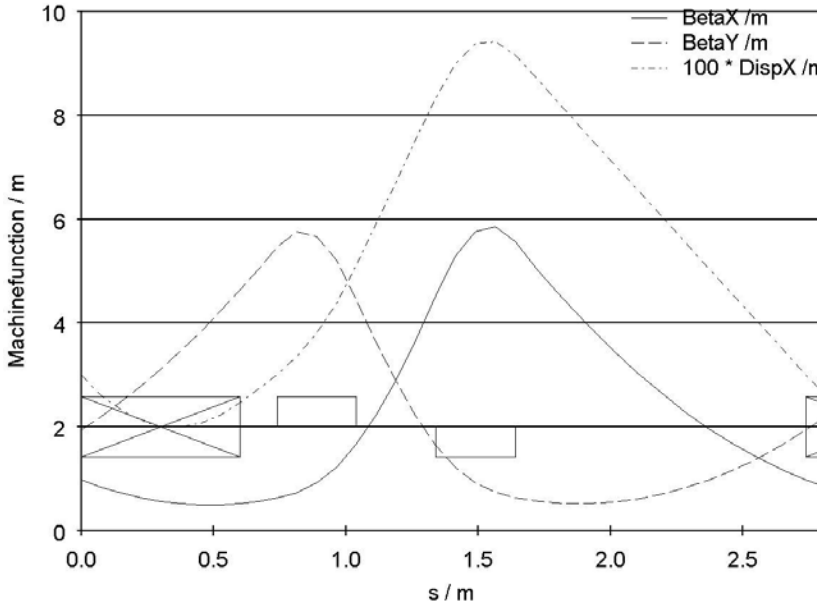

Figure 5: Machine functions of BEP-like structure. Maximum value of dispersion function is ~9.5cm.

This structure gives $Q_x \cong 23.7$, $Q_y \cong 22.7$, $\tau_y \cong 3.7$ms. For RF voltage ~1.2 MeV $\sigma_s \cong 0.87$ cm. Beam lifetime for 10^{10} particles is ~7.47s. For mechanical coupling $\kappa_0 \cong 0.01$, vertical invariant emittance goes to be $\sim\varepsilon_y \cong 7.4 \cdot 10^{-10}$ m rad. Other parameters are represented in Table 5.

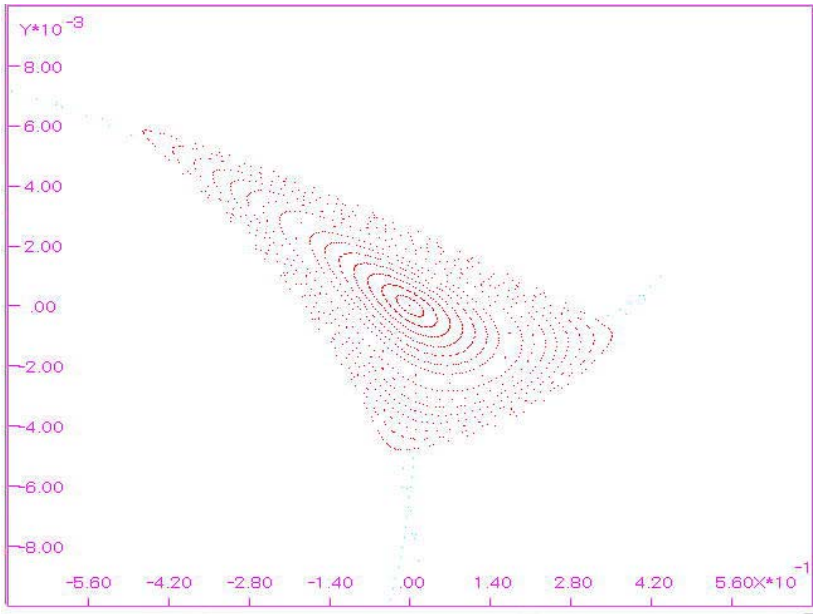

Figure 6: Phase space portrait at the magnet entrance. Abscissa represents x, cm, ordinate x' rad, respectively.

Chasman-Green type structure

Symmetrical structure with minimal dispersion in the middle considered in [16]. Mechanical view is represented in Figure 4. Here as in previous structures the thick plate carries all focusing elements.

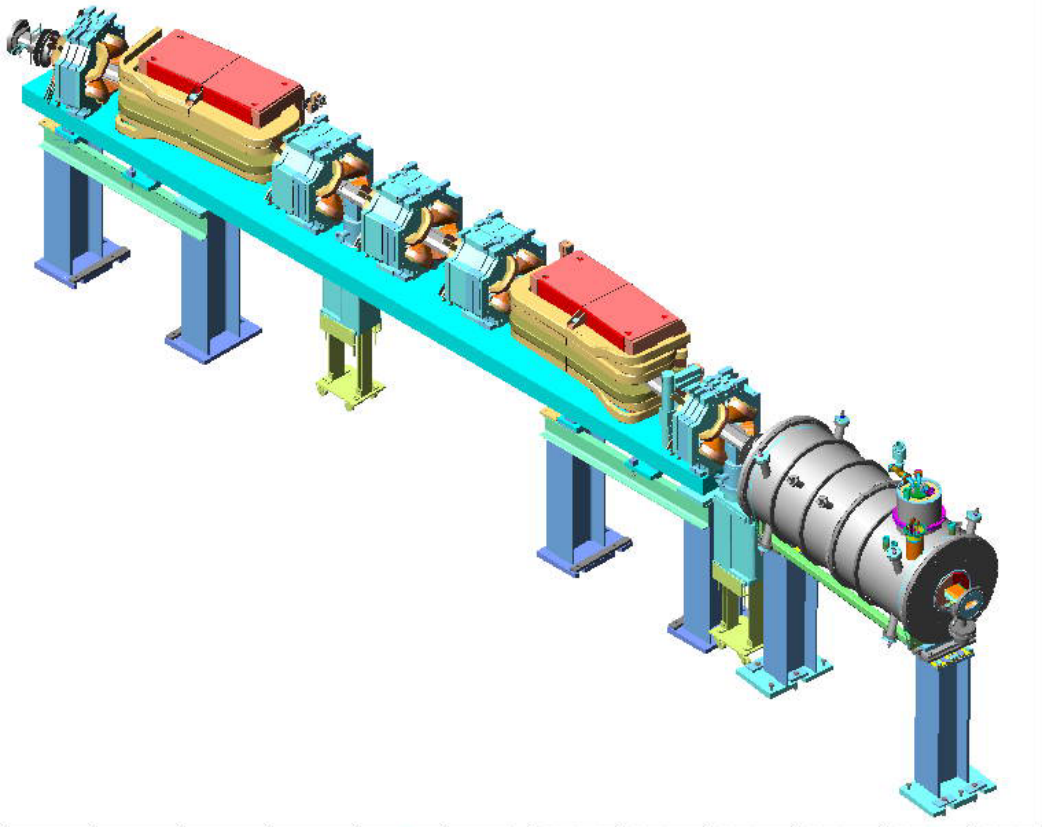

Figure 7: Mechanical realization of Chasman-Green like structure period.

Table 4.

Energy	~2.8 GeV
Length of magnet	60 cm
Field in magnet	~12.1 kG
Length of defocusing quad	20cm
D Gradient	~ -7.6
Sextupole in lens	~ -1.9 kG/cm^2
Length of centr. focusing quad	20 cm
F gradient 1	~13.5 kG/cm
Sextupole in lens	2.12 kG/cm^2
Length of inner. Focusing quad	20 cm
F gradient 2	~-4.5 kG/cm
Sextupole in lens	0
Wiggler period	10 cm
Number of poles	9
Perimeter	~168 m
Number of periods	40

Central lens can be increased in length, so gradient can be decreased proportionally.

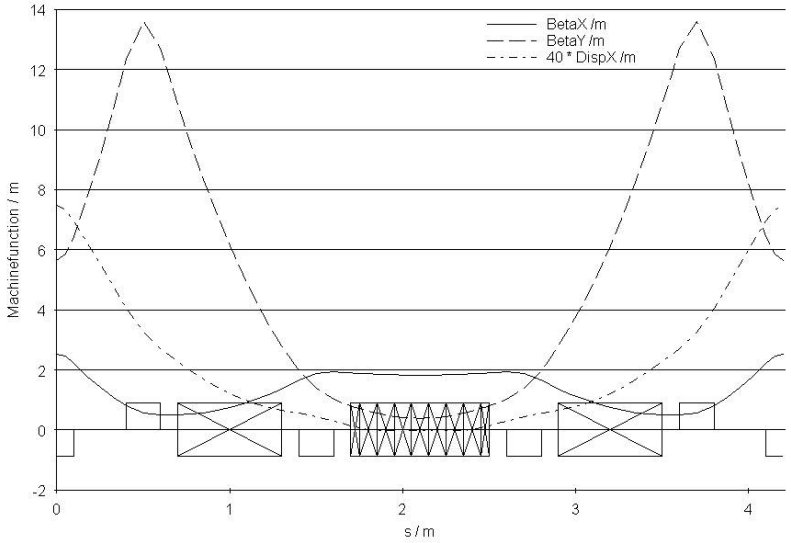

Figure 8: Example of machine functions of Chasman-Green like structure. Maximum value of dispersion function is ~20cm.

The structure operates at $Q_x \cong 24$, $Q_y \cong 12$, $\tau_y \cong 1.5$ms. For RF voltage ~2.5 MeV $\sigma_s \cong 0.26$ cm. Beam lifetime for mechanical coupling $\kappa_0 \cong 0.02$ and 10^{10} particles is ~700s. Vertical invariant emittance goes to be $\sim \varepsilon_y \cong 3 \cdot 10^{-9}$ m rad. Other parameters are represented in Table 5.

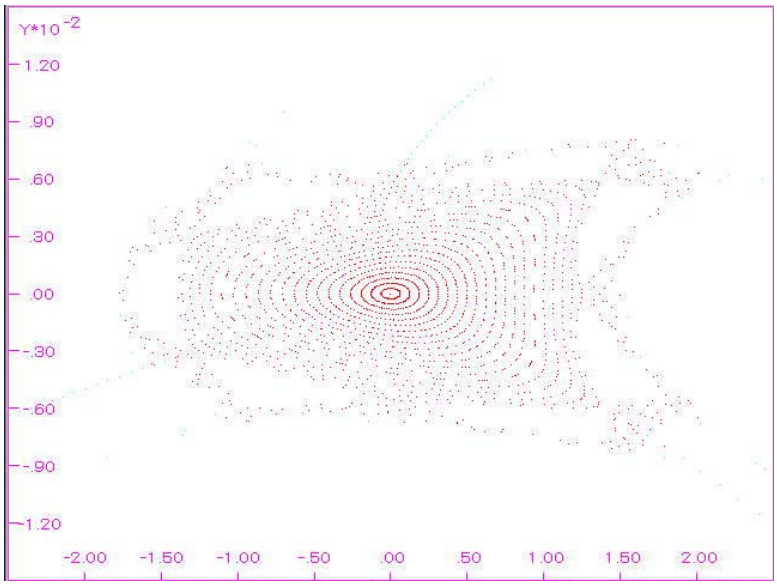

Figure 9: Phase space portrait in the middle of central focusing lens. Abscissa represents *x*, cm ordinate x' rad, respectively.

For calculation the wiggler poles suggested as a sector ones, so the vas no problems with fringe focusing. Making poles with angles can be accepted if the wiggler field is fixed, so the wiggling trajectory is fixed also.

View of machine functions in Fig. 8 is extremely sensitive to exact values of gradients in lenses.

This structure includes significant wiggler length. Each wiggler, a 9-pole one has tapering at the ends in ¼, ¾ of maximal value, which is 24 kG. This made for elimination of average displacement of dispersion functions in wiggler. The very edge poles made of 5 cm long with ~twice higher field for more compact size. So total length of wiggler cold mass goes to be~80 cm-long. If wigglers installed in every straight section, the total length going to be ~32 meters only. All these wigglers plus magnets give damping $\tau_y \cong 1.5$ms –much smaller, than required, so some of the wigglers can be omitted. This space can be used for injection/extraction, RF cavities and so on. The field in the wigglers can be reduced also.

Wiggler with similar parameters was developed for CESR [17]. It was shown in [17], that physical nature of appearance of octupole (and higher) type dependence of kick versus vertical displacement is in *wiggling with angle in fringe sextupole* (and higher) field, as the fringe longitudinal field of any multipole has a structure of next order multipole. The sextupole generated intrinsically by the field variation in longitudinal direction (along the wiggler). When the pole is wide, the sextupole has strict value defined by second derivative of the wiggler field *along* the longitudinal coordinate *s*. For a pole with finite width the real sextupole adds (or subtracts) to the intrinsic one.

So this structure looks not bad, however the big point of concern is the accuracy of field modeling. In some publications authors claim, that they proposed good algorithm for tracking through the wiggler field. On the pictures representing outer angle as function of input coordinate mostly of these algorithms give symmetrical function. Meanwhile simple general considerations show that this is not possible. Really let us suggest for simplicity that all inner poles are infinitely wide and end poles only have significant roll-off. Suggest further, that for incoming particle exactly with zero transverse coordinate and angle outer coordinate and angle are adjusted to be zero too. Let now consider two particles entering the wiggler's first pole with equal absolute value of displacements, but from opposite sides around center. In this case both particles acquire ~the same addition angle inside the wiggler in direction opposite to the kick given by this end pole. In the last pole these two particles will acquire different angles, which are not symmetrically distributed around zero value. Even and odd pole number wigglers have these outer functions with mirror symmetry. Parameterization in the models mentioned requires hundred parameters for typical case. It someone decide to take into account imperfections of fabrication, this number grew tens times. Evidently results of calculations will be under serious doubt.

So desire to have the structure as simple as possible is natural respond to complexity of task. Especially as only the vertical emittance plays decisive role.

Meanwhile this type of considerations can be useful for CESR future. After the charm physics accomplished, all 18 SC wigglers can be distributed evenly around the ring appropriately surrounded by quadrupoles. About 36 new quads required for obtaining the structure view just described, (one can look at Fig. 7 and keep in mind CESR's magnets instead of drawn ones). This will bring " bright" future for CESR as a light source.

Coming back to the structure, one can see that this structure gives increased vertical emittance, however. Mechanism is the following. This structure has very low compaction factor, $\alpha \cong 0.0003$. So the beam is short enough, which yields intensive IBS with heating vertical emittance.

Concluding we can stress once again that IBS approximately gives factor 2-4 in emittance. For energy below 2 GeV this increase will be much higher.

In Table 5 all these structures represented in comparison.

Table 5.

Parameter	FODO	BEP	CH-GR
Energy, MeV	~3	~3	~3
Perimeter, m	160	181	152
Number of periods	50	66	40
Moment compaction factor	0.00178	0.0007	0.0003
Q_x	15.54	23.4	~24.
Q_y	15.49	22.3	~12.
J_x	1.914	0.99	2.002
J_y	1.086	2.01	0.74
τ_z , ms	2.7	3.5	.74
$\varepsilon_{x,\gamma}$, cm rad $/10^{-3}$	1.97	1.1	0.42
$\varepsilon_{x,IBS}$, cm rad $/10^{-3}$	2.57	3.3	1.88
$\varepsilon_{x,Itot}$, cm rad $/10^{-3}$	4.55	4.5	1.5
ε_y , cm rad $/10^{-7}$	0.86	0.74	3.0
$U_{RF,}$ MV	2.0	1.5	2.5
Frequency of RF, MHz	~700	~700	~700
$\Delta E / E$	0.0051	0.0057	0.026
$(\Delta E / E)_\gamma$	0.0014	0.001	0.0016
$(\Delta E / E)_{tot}$	0.0016	0.0010.0133	0.0017
σ_s , cm	0.98	0.87	0.25

One can see, that vertical normalized emittance is about the same in all structures.

SPIN DYNAMICS

Polarization recognized as a powerful tool for the High Energy Physics. In NLC project the electron beam is polarized from the beginning of its journey. Now even positron bunch polarization option is under consideration for NLC. For VLEPP project all beams supposed to be polarized from the very beginning. So handling spin in the ring is a matter of highest priority. Fortunately processes of polarization/depolarization are much slower, than radiation damping, however some attention required here. First, the energy of the ring must be chosen so that spin revolution frequency is sitting at half integer spin resonance. The last defined by the energy of the ring to be an integer number of 440.65 MeV plus half of this. This is about 2864.22 MeV or 3304.8 MeV for the subject of our interest. Formulas and the lattices evaluations remain valid, despite the slight difference in energy value.

Characteristic time of polarization in magnetic field is [18]

$$\tau_p \cong \frac{8}{5\sqrt{3}} \frac{\alpha}{r_0^2 \gamma^5 c} \frac{1}{\left\langle \frac{1}{|\rho|^3} \right\rangle}, \tag{36}$$

while the time of radiation damping is (9)

$$\tau_s \cong \frac{3}{2}\frac{1}{r_0 \gamma^3 c\left\langle \frac{1}{\rho^2} \right\rangle}, \tag{37}$$

So the ratio of damping time to the time of polarization can be expressed as

$$\frac{\tau_p}{\tau_s} \cong \frac{16}{15\sqrt{3}}\frac{\alpha}{r_0 \cdot \gamma^2}\frac{\left\langle \frac{1}{\rho^2} \right\rangle}{\left\langle \frac{1}{|\rho|^3} \right\rangle} \approx \frac{\alpha\rho}{r_0\gamma^2}. \tag{38}$$

First if average of $\left\langle \frac{1}{|\rho|^3} \right\rangle = 0$, then equilibrium value of polarization is zero. This situation realized, for example in a wiggler dominant machine if wiggler has even number of poles. Formula (38) yields for $\rho \cong 6\text{m}$, $\gamma \cong 6000$, the ratio goes to

$$\frac{\tau_p}{\tau_s} \approx 3 \cdot 10^5,$$

so for $\tau_s \approx 2 \cdot 10^{-3}$ s, (de)polarization time goes to $\sim \tau_p \cong 6\ 10^2$ s, i.e. ~10 min. During this time, together with short beam lifetime itself, it is necessary to make measurements of polarization in a ring to be sure, that it has desirable value and so on. Reducing the number of particles helps in extending the lifetime,

LINEAR DAMPING SYSTEM

Extreme development of damping ring emerges a Linear Damping System [19], what can be considered as straightened ring. (LDS) is a sequence of wigglers and accelerating structures, installed along a straight line. Here in [19] the losses in wigglers ~ 1MeV/cm are compensated by RF accelerating structures with the same rate of energy gain. Particle here must re-radiate all its initial energy similarly as it is going in any circular damping ring. But the system of wigglers and cavities aligned along straight line here and that system cooled the bunch by single pass keeping the average energy of the bunch constant. To keep so high losses high energy required.

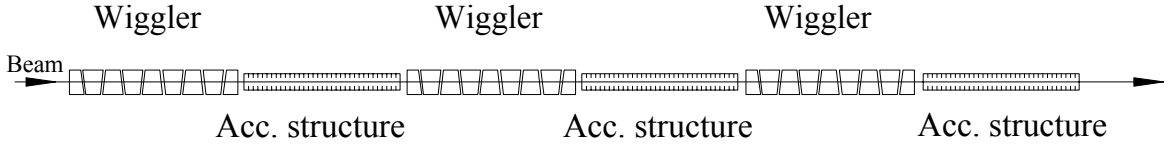

Figure 5: Linear Damping System [19]. Accelerating structures aligned with wigglers. The rate of losses in the wiggler is the same as the acceleration in RF structures, so the energy of the beam ~const. In principle, the accelerating structures can be located between the poles of wigglers.

LDS was introduced in attempt to have the dispersion invariant as low as possible. Instead of damping time so-called characteristic-damping length emerges, defined as

$$l_s = -\frac{\gamma}{d\gamma/ds} = \frac{3}{2}\frac{\lambda_W^2}{r_0 K^2 \gamma}. \tag{36}$$

where $K = \frac{eH\lambda_W}{mc^2}$ One can see that $1/l_s$ has *linear* dependence on energy.

For a dipole wiggler, the periodic solution for η_x can be expressed as [3]

$$\eta_x = \frac{K_x \lambda}{\gamma} Sin\frac{s}{\lambda} = \frac{\lambda^2}{\rho_x} Sin\frac{s}{\lambda}, \tag{37}$$

where $\rho_x = \lambda\gamma / K_x$ is the bending radius in magnetic field of the wiggler. The length of formation of radiation is $\rho_x / \gamma = \lambda / K_x$.

For the function H_x we can estimate $H_x \cong \beta_x \eta_x'^2$. As the $\eta_x' \cong K_x / \gamma \cdot Cos(s/\lambda)$ one can obtain

$$H_x \cong \beta_x K_x{}^2 / \gamma^2 \cdot Cos^2(s/\lambda).$$

So formula (14) becomes

$$\frac{d\varepsilon_x}{ds} = \left\langle \left(1 + K_x^2 Cos^2(s/\lambda)\right)\frac{\beta_x}{\gamma^2}\frac{d(\Delta E/E)^2_{tot}}{ds} \right\rangle - 2\alpha_x \varepsilon_x \tag{38}$$

For vertical emittance $K_x = 0$ (and the wiggler field has no horizontal polarization). Equilibrium emittances defined by condition $d\varepsilon_{x,y}/ds = 0$. For quantum excitation the source in (38) does not depend on emittance. So for quantum excitation (38) yields

$$\varepsilon_x \cong \tfrac{1}{2}\cdot\lambda_C \overline{\beta}_x \left(1 + K_x^2/2\right)\cdot\gamma/\rho_x \cong \tfrac{1}{2}\cdot\lambda_C \overline{\beta}_x \left(1 + K_x^2/2\right)K_x/\lambda_W \tag{39}$$

$$\varepsilon_y \cong \tfrac{1}{2}\cdot\lambda_C \overline{\beta}_y \gamma/\rho_x \cong \tfrac{1}{2}\cdot\lambda_C \overline{\beta}_y K_x/\lambda_W, \tag{40}$$

where $\overline{\beta}_{x,y}$ – are averaged envelope functions in the wiggler. The last formulas together with (36) define the cooling dynamics under SR. One can see that equilibrium invariant emittances *do not depend on energy*. In addition, quantum equilibrium *vertical emittance* and the cooling time do not depend on the wiggler period at all. Substitute for estimation $\overline{\beta}_{x,y} \approx 1m,\ \lambda \cong 5cm$, $K \cong 5$, one can obtain for *quantum emittances* the following estimations for equilibrium invariant emittances

$$\varepsilon_x \cong 2.5\cdot 10^{-8} cm\cdot rad, \tag{41}$$

$$\varepsilon_y \cong 9.5\cdot 10^{-10} cm\cdot rad. \tag{42}$$

For IBS scattering considerations show, that there is real coupling similar to what happens in ordinary damping ring as the following

$$\left(1 + K_x^2/2\right)\frac{\varepsilon_y}{\beta_y} = \frac{\varepsilon_x}{\beta_x}, \tag{43}$$

i.e. vertical temperature is $\sim K^2$ times smaller, than radial. This type of post-cooler might be important in TeV scale machines giving post-cooling damping.

[3] AS we mentioned, the wiggler must have the ending field in poles relation as ¼, -¾, 1, n(-1,1), - ¾ , ¼ . n=0,1,... This will give ~zero averaged displacement of trajectory [10].

COMPARISON WITH PRESENT NLC DESIGN

Let we take for comparison present NLC design [8] and, say, FODO lattice described above. Optics of FODO structure is slightly massaged for better performance. Perimeters of the ring also changed to accommodate two of NLC linac trains by 192 bunches with 1.4-ns spacing, ($\cong$ 80.16 meters) giving kicker's rise/fall time sum 20 ns, what requires additional 40 ns or ~ 12 meters extra to the perimeter. This will add 8 periods to the ring. This lens can also be added by slight increase in length of straight sections in period, 24 cm total. In this ring, the damping can be easily improved by slight gain in operational energy. In this case the only single train can be carried in the ring. Parameters of the ring in comparison with proposed parameters from [8] are represented in Table 6.

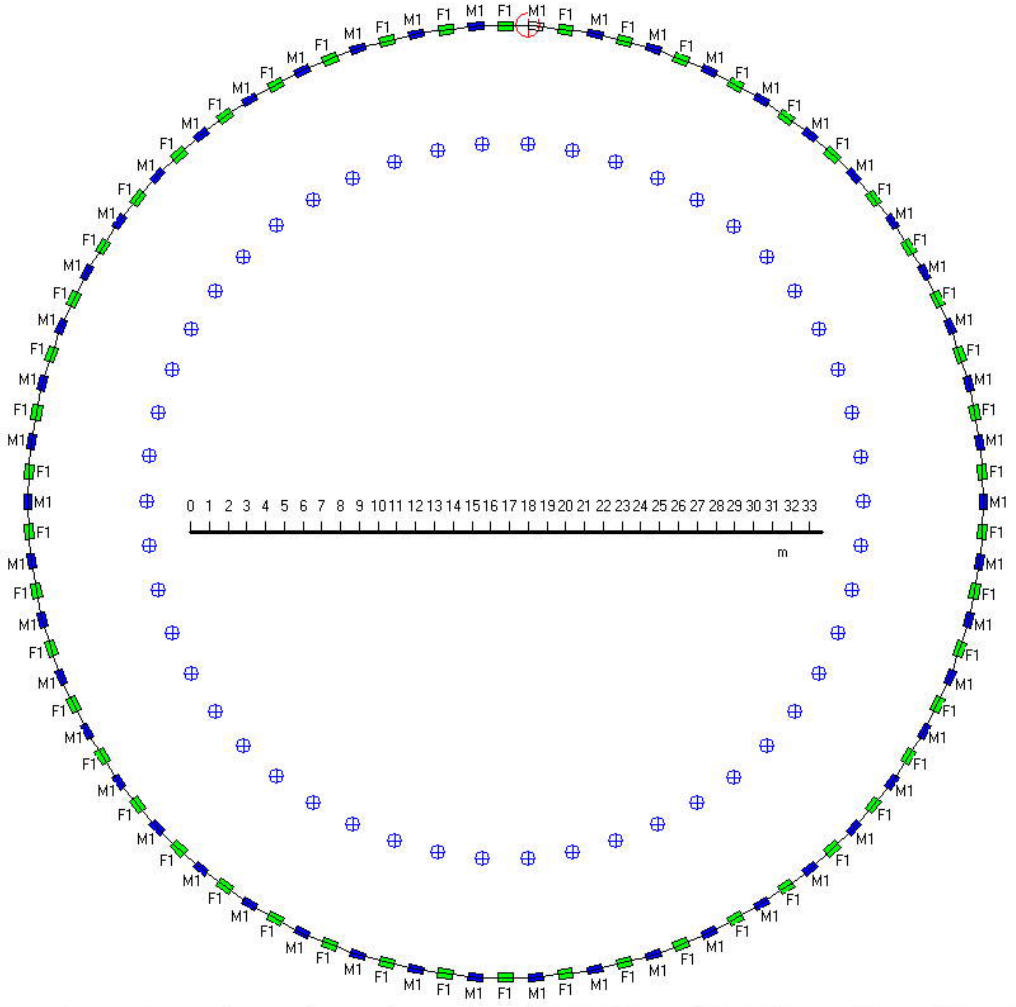

Figure 10: Top view on the FODO ring. Circled crosses mark centers of bending radiuses. Scale at the right low given in meters, so average radius ~25.5 m. Dots represent the centers of bending magnets.

Top view on the ring is rather trivial, however it gives an idea of possible alignment procedure. Each Al block can be installed on stabilized platform, as it was done for JLC test facility damping ring [20].

Table 6.

Parameter	Units	[8], Feb.2003	This paper
Energy	E/GeV	1.98	3.304
Number of bunch trains	N_{train}	3	2
Circumference	C /m	299.79	185.6
Arc cell type		TME	FODO
Arc cell length	/m	5.12	3.2
Length of wiggler straights	/m	2×49.297	0
Length of injection straights	/m	2×22.468	0.8
Number of arc cells		28+8×½	58
Main arc dipole field	/T	0.67	1.49
Main arc dipole gradient	K_1 /m	-0.315	-1.7
Betatron tunes	Q_x, Q_y	21.15, 10.347	~18/18.
Natural chromaticity	ξ_x, ξ_y	-30.74, -28.76	-27.57, -27.66
Normalized natural quantum emitt.	$\gamma\varepsilon_0$ /μm rad	2.37	4.2
Damping times	τ_x, τ_y, τ_ε /ms	3.63, 4.08, 2.08	1.49, 2.86, 2.64
Extracted horizontal quantum emitt.	$\gamma\varepsilon_{x,ext,\gamma}$ /μm rad	2.37	5.1
Extracted horizontal total emittance*	$\gamma\varepsilon_{x,ext,tot}$ /μm rad	Not calculated	8.1
Extracted vertical quantum emitt.	$\gamma\varepsilon_{y,ext,\gamma}$ /μm rad	0.02	0.00089
Extracted vertical total emittance*	$\gamma\varepsilon_{y,ext,tot}$ /μm rad	Not calculated	~0.001
Momentum compaction	α	0.001388	0.001312
RF frequency	f_{RF} / MHz	714	~700
RF voltage	V_{RF} /MV	2.0	2.5
Number of RF cavities		5	5
RF acceptance	ε_{RF} /%	1.52	1.61
RMS energy spread	σ_δ /%	0.0975	0.136*
Natural quantum bunch length	σ_z / mm	5.49	6.5
Total bunch length	σ_z / mm	Not calculated	6.6*
Synchrotron tune	Q_s	0.0118	0.0072
Wiggler peak field	$\hat{B}_w$ /T	2.15	No Wiggler
Wiggler period	λ_W /m	0.27	No Wiggler
Wiggler total length	L_W /m	61.568	No Wiggler
Integrated wiggler field	$\int \hat{B}_W^2 ds$ T^2m	168.1	No Wiggler
Energy loss/turn from dipoles	U_0 /keV	136	1397
Energy loss/turn from wigglers	U_W /keV	834	No Wiggler
Total energy loss/ turn	U_0+U_W /keV	970	1397
Energy loss ratio	U_W/U_0	6.13	0
Beam lifetime for N_{bunch}=5 10^{10}	τ_{IBS} / s	Not calculated	2357
Lifetime of polarization	τ_{pol} /s	Not calculated	∞

* - Number of particles per bunch N_{bunch}=5 10^{10} . This number is not specified in [8].

The energy chosen here is highest possible; other point is 2864 MeV looks also acceptable. According to (5) luminosity can be achieved with N=10^{10}, f=120 Hz $\Delta E / E \cong 0.1$ is $L \cong 1.0 \times 10^{34}\,\mathrm{cm}^{-2}\mathrm{s}^{-1}$. Coupling remains about ten times higher than minimal possible limit arising from IBS.

CONCLUSION

Materials represent in this publication supposed to open the case about damping ring design for NLC. Previous publications made by SLAC/LBL team look not adequate to the high price of future Linear Collider. Especially this is true for IBS considerations.

More simple schemes look more guaranteed for this purpose. Important role belongs to the physical considerations (as always). Results of [10] can be useful for design of damping ring for NLC. Fundamental difference between existing proposal and the one forwarded in this publication is in higher energy of the ring, up to 3-3.5 GeV and in illuminating the dominant importance of vertical emittance. Higher energy allows, first, to reach necessary damping without wigglers and, second, significantly improves situation with IBS. Equilibrium spin orbit is less important, but adds to advantages of FODO-like structure too. This structure is absolutely symmetric, what makes the tuning and alignment much more simpler too.

Ideas about these types of structures were under discussion at BINP, Novosibirsk starting at ~1980, see [7] for references. Similar idea about damping ring design as a FODO type was published in [21]. Here authors also found ~12.3 GeV optimal for combined function FODO cell[4].

Considerations represented above done for the room temperature option of Next Linear Collider. Although SC version has significantly different scale and requirements, physical consideration illuminated in this paper are applicable to that option in full too.

REFERENCES

[1] U.Amaldi, “A possible Scheme to obtain e^-e^- and e^+e^- collisions at Energies of hundreds of GeV”, Phys. Let., Vol. 61B, N3, pp.313-315(1976).

[2] K. Steffen, “ The Wiggler Storage Ring, a Device with Strong Radiation Damping and Small Beam Emittance”, DESY PET-79/05, Feb. 1979, 9pp.

[3] P. Krejcik, “Design for a Practical, Low emittance Damping Ring”, Proc. EPAC-Conf., Rome, Vol.1, p. 752 (1988).

[4] L. Smith, “Effects of Wigglers and Undulators on Beam Dynamics”, LBl-21391 (1986) and presented at the XIII Int. Conf. on High Energy Acc., Novosibirsk, USSR (1986).

[5] T. Raubenheimer, W.E. Gabella, P.L. Morton, Martin J. Lee, L.Z. Rivkin, R.D. Ruth, “A damping ring design for future linear colliders”. (SLAC). SLAC-PUB-4912, Mar 1989. 3pp.

[6] T.O. Raubenheimer, L.Z. Rivkin, R.D. Ruth, ” Damping Ring Designs for a TeV Linear Collider”, SLAC-PUB-4808, Dec. 1988, Contributed to DPF Summer Study Snowmass’88, Snowmass, CO, June 27-July 15, 1988.

[7] V.V. Anashin, I.B.Vasserman, V.G.Veshcherevich, B.I. Grishanov, I.A. Koop, V.I. Kupchik, I.G. Makarov, A.A. Mikhailichenko, O.A. Nezhevenko, V.N. Osipov, E.A. Perevedentsev,

[4] Cell here has bending fields in both magnets. Radius of machines considered was 100 and 300 m. Straight sections were ~24 cm only, however.

V.M. Petrov, I.K. Sedlyarov, A.N. Skrinskii, E.M.Trachtenberg, Yu.M. Shatunov, V.P. Yakovlev, " Prototypes of the Damping Ring and the Buncher for the VLEPP Project", XIII International Conference on High Energy Accelerators, Novosibirsk, USSR, Aug 7-11, 1986, pp 159-163. By. SLAC-TRANS-0224, Oct 1986. 14pp. Published in Novosibirsk Accel.1986 v.1:159 (QCD183:I5:1986).

[8] M. Woodley, A. Wolski," The NLC Main Damping Ring Lattice", LCC-0113, CBP Tech Note-276, February 2003.

[9] A.A. Mikhailichenko, "Damping Ring for VLEPP linear collider", III international Workshop on linear Colliders LC91, Protvino, September 17-27, 1991. Proceedings, Edited by V.E. Balakin, S. Lepshokov, N.A. Solyak, Serpukhov, (IFVE). 1991. Serpukhov, USSR: BINP (1991).

[10] A. Mikhailichenko, V.V. Parkhomchuk, " Damping Ring for Linear Collider", BudkerINP 91-79, Novosibirsk, 1991.

[11] A. Mikhailichenko, "On the physical limitation to the lowest emittance (toward colliding electron- positron crystalline beams)", 7th Advanced Accelerator Concepts Workshop, 12-18 October 1996, Lake Tahoe, CA, AIP Conference Proceedings 398, p.294: CLNS 96/1437, Cornell, 1996.

[12] A.A.Mikhailichenko, "A Beam Focusing System for a Linac Driven by a Traveling Laser Focus", PAC95, Dallas, TX, Proceedings, p. 784 (RAB018).

[13] H. Bruck, "Accèlèrateures Circularires de Particules", Press Universitaures de France, 1966.

[14] B.Touchek, "Physics with Electron Storage Rings", V Internat. Conference on Hogh Energy Accelerators, Frascati, 1965, p.263.

[15] A. Piwinsky, *IBS,* Proc. 9th Intern. Conf. on High Energy Acc., Stanford, CA, 2-7 May, 1974, SLAC, 1974.-p. 405.

[16] R. Chasman, K.Green, "Proposal for a National Synchrotron Light Source", BNL, 50595, 1977.

[17] A. Mikhailichenko, "Optimized Wiggler Magnet for CESR", PAC2001, Chicago, IL, June 18-22, 2001, Proc., pp. 3648-3650.
A. Mikhailichenko, "The Wiggler for a Damping Ring", LC02, Feb. 4-8, SLAC, Stanford, CA, 2002.

[18] A.A. Sokolov, I.M. Ternov, Sov. Phys. Dokl., **8**,1203(1964).

[19] N.S. Dikansky, A.A. Mikhailichenko, "A linear Damping System for Obtaining High Energy $e^{\pm}$ with extremely low Emittance ", EPAC 92, Berlin, 1992, Proc., p.898; Preprint BINP 88-9, Novosibirsk, 1988.

[20] ATF Test facility, KEK, 1995.

[21] L. N. Hand, S. Lundsgren," The Design of Low Emittance Electron Storage rings". CLNS 88/841, May 1988.